Applied Catalysis B: Environmental 134–135 (2013) 231–237

Contents lists available at SciVerse ScienceDirect

Applied Catalysis B: Environmental

journal homepage: www.elsevier.com/locate/apcatb

On the role of the activation procedure of supported hydrotalcites for base catalyzed reactions: Glycerol to glycerol carbonate and self-condensation of acetone

M.G. Álvarez[a,b], A.M. Frey[c], J.H. Bitter[c], A.M. Segarra[a,b], K.P. de Jong[c], F. Medina[a,b,*]

[a] Department d'Enginyeria Química, Universitat Rovira i Virgili, PO Box 43007, Tarragona, Spain
[b] EMaS – Centro de Investigación en Ingeniería de Materiales y micro/nano Sistemas, PO Box 43007, Tarragona, Spain
[c] Department of Inorganic Chemistry and Catalysis, Debye Institute, Utrecht University, PO Box 80 083, 3508 TB Utrecht, The Netherlands

ARTICLE INFO

Article history:
Received 12 November 2012
Received in revised form 7 January 2013
Accepted 11 January 2013
Available online 18 January 2013

Keywords:
Supported hydrotalcite
Carbon nanofibers
Glycerol
Glycerol carbonate
Transesterification
Aldol condensation
Polarity

ABSTRACT

Bulk and carbon nanofiber supported MgAl hydrotalcites have been investigated as solid base catalysts for the synthesis of glycerol carbonate and dicarbonate and for the self-condensation of acetone. The supported materials exhibited a 300 times higher activity compared to bulk activated hydrotalcites for the transesterification. The materials could be reused while maintaining a high yield of glycerol carbonate. The activity of the mixed oxide, i.e., hydrotalcite materials after high temperature activation was considerably higher than both gas-phase and liquid phase rehydrated samples for the glycerol reactions. In contrast in the acetone self-condensation reaction the rehydrated samples were more active. This indicates that the polarity of the catalyst related to the reactant properties has a huge impact on the performance of a solid base catalyst.

© 2013 Elsevier B.V. All rights reserved.

1. Introduction

Glycerol is produced in large quantities as a by-product in the biodiesel production. A commercialization of glycerol will increase the profitability of producing biodiesel. The increased glycerol supply, due to the increasing biodiesel production, is pushing the glycerol price down. This makes it even more attractive to explore strategies for transforming it into more valuable products. Several of such conversion processes are described in the literature [1], such as: ketomalonic acid by selective oxidation, fuels oxygenate by etherification [2,3] or by acetylation [4], propyleneglycol by hydrogenolysis, acrolein by dehydration [5], highly branched polymers by esterification, synthesis gas by reforming [6,7]. Glycerol carbonate is one of the glycerol derivatives finding increasing interest in the chemical industry [8–12] and has potential as a novel component of gas-separation membranes [13] or biolubricant. Glycerol carbonate can furthermore be used for the synthesis of new functionalized polymers such as polyesters, polycarbonates or polyurethanes that might find interesting new applications [14–16]. Likewise, it may be used in the synthesis of intermediates such as glycidol [17] or as solvent for coatings, cosmetics, personal care, and detergents.

One of the simplest methods to obtain glycerol carbonate is by the transesterification of glycerol with a dialkyl carbonate (Scheme 1). Transesterification reactions can be carried out both under basic and acidic conditions; however, the conversion in this reaction using acidic catalysts is lower than that of the base catalyzed reaction [18]. Base catalysis seems more promising and has been investigated more. Within base catalysis solid bases are in particular interesting due to the fact that they can easily be re-used. Furthermore corrosion problems and waste productions i.e., salt formation are avoided.

One important group of solid base catalysts are the hydrotalcites (HT). Hydrotalcites are anionic clays which have the general formula $[M_n^{2+}M_m^{3+}\ (OH)_{2(n+m)}]^{m+}\ A_{m/n}^{x-}\cdot yH_2O$, where M^{2+} and M^{3+} denote a divalent and a trivalent cation, respectively, and A^{x-} is a charge compensating anion. This structure consist of brucite-like layers $[Mg(OH)_2]$ in which magnesium cations are in the centre of octahedrons and hydroxyl groups are in its vertices and are connected forming layers. In HT, some divalent cations are substituted by trivalent cations introducing a positive charge, which is balanced by anions located in the interlayer. Additionally, crystallization water molecules are also found in the interlayer. Changing the synthesis conditions can vary the lateral size of the layers and

* Corresponding author.
E-mail address: francesc.medina@urv.cat (F. Medina).

0926-3373/$ – see front matter © 2013 Elsevier B.V. All rights reserved.
http://dx.doi.org/10.1016/j.apcatb.2013.01.011

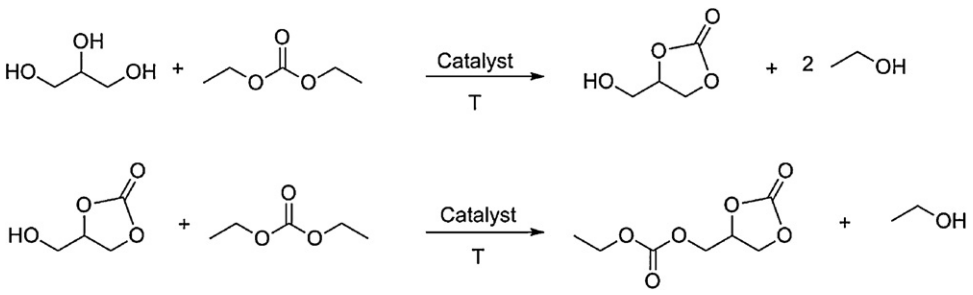

Scheme 1. Consecutive hydrotalcite-catalyzed transesterification reaction of glycerol with DEC.

the degree of stacking [19]. Thereby the properties of the catalyst can be varied.

Previous studies show that hydrotalcites (mixed oxides and its rehydrated forms) are efficient and reusable catalysts for the transesterification reaction, and might potentially after further optimization be an alternative to catalysts such as K_2CO_3 [20]. Takagaki et al. showed that an uncalcined hydrotalcite containing a hydromagnesite phase efficiently catalyzes glycerol carbonate synthesis from glycerol and DEC using DMF as solvent [21].

The controlled decomposition of precipitated hydrotalcite-like compounds by calcination leads to a high surface areas mixed oxide which exhibit Lewis basicity and can be used as catalysts or catalytic supports in a great variety of reactions [12,22,23]. The acid-base properties of calcined hydrotalcites can be modulated by changing the calcination temperature, the nature and amount of structural cations and also of the anions which are compensating the positive charge, as well as the preparative method [13,19,23]. The generated oxides shows a characteristic "memory effect", meaning that the material can recover its original hydrotalcite structure by rehydration. By rehydration either in liquid phase or in gas phase the oxide originating from a hydroxycarbonate is converted to its topotactic rehydrated hydroxide having the same structure as the parent material but has different anions between the layers. The rehydrated materials contain Brønsted basic sites [24,25] due to the presence of OH^- as compensating anions in the interlayer space. This makes them useful for a wide number of base-catalyzed reactions using such sites such as Knoevenagel and Claisen-Smith condensations [26,27], Michael additions [28] or transesterification reactions [29,30].

Roelofs et al. [31] have found that the active sites on hydrotalcites are likely located at the edges of the platelets, representing only a minor part of the Brønsted-sites in the hydrotalcite. Several attempts have been made to increase the number of active sites [25,32,33], however the exposed edge area is limited by the lateral size of HT crystallites. The size can be varied by using different synthesis methods and ageing temperatures [25] or by applying ultrasound during synthesis or rehydration [31,32]. By depositing small hydrotalcite nanoparticles (~20 nm) on carbon nanofibers solid base catalyst the HT weight based activity for acetone self condensation increased by a factor 10 compared to bulk HT. The increase in activity is due to the higher amount of accessible sites [34,35]. We report here a study of the performance of such carbon nanofibers supported hydrotalcites in the transesterification of glycerol with diethyl carbonate, which are up to 300 times more active than bulk hydrotalcites. We evaluate furthermore the activity of mixed oxides versus the rehydrated samples and the influence of the reconstruction method (liquid-phase versus gas-phase rehydration). We compared the difference in activity profile between mixed oxide and rehydrated samples in this reaction with the performance of the same catalysts in the self-condensation reaction of acetone to diacetonealcohol.

2. Experimental

2.1. Catalysts preparation

Hydrotalcite supported on CNF (Mg/Al = 2) was prepared as follows: magnesium and aluminium (with a molar ratio 2:1) was introduced on 5 g of oxidized carbon nanofibers (prepared as described elsewhere [32,33]) by incipient wetness impregnation of an aqueous solution of the corresponding nitrates (0.7 cm^3/g) in such a way that a loading of 12 wt% of HT was obtained. The material was kept at room temperature for 1 h for equilibration and was then dried at 393 K for 2 h in static air. A second impregnation step with a base solution (containing 8.3 M NaOH and 0.56 M Na_2CO_3) was performed. The resulted material was aged for 18 h at 333 K in a water saturated N_2 atmosphere, followed by washing with deionised water (3×20 cm^3). Finally, the sample was dried at 393 K for 12 h and sieved to a fraction of 20–150 micron.

Unsupported hydrotalcite with a Mg/Al molar ratio of 2 was prepared by coprecipitation of magnesium and aluminium nitrates at a constant pH as described below. The appropriate amounts of $Mg(NO_3)_2{\cdot}6H_2O$ and $Al(NO_3)_3{\cdot}9H_2O$ were dissolved in 150 cm^3 of distilled water and added dropwise into a glass vessel which initially contained 200 cm^3 of deionized water. The pH was controlled and kept at 10 by adding a 2 M NaOH solution. Both solutions were mixed under vigorous stirring and the suspension was stirred overnight at room temperature. The precipitated solid was filtered and washed several times with water and dried at 383 K to yield the parent hydrotalcite.

Activation of the Mg/Al supported hydrotalcite (HT-CNF) was performed by either thermal decomposition in Ar by heating at 10 K/min up to 773 K (denoted below as HT-CNFc) for 3 h or by calcination followed by rehydration under inert atmosphere in either liquid or gas phase. For rehydration in liquid phase, 0.3 g of HT-CNFc sample were dispersed into 10 cm^3 of deionised and decarbonated water and stirred over 24 h at room temperature. The catalyst was separated by centrifugation, washed with ethanol and dried at 373 K under inert atmosphere for 15 h. The sample was denoted as HT-CNFrl. The rehydration in gas phase was performed as follows. The as-synthesized HT-CNF sample was heated under an Ar flow to 723 K with a rate of 10 K/min for 3 h. Then, the sample was rehydrated by passing a flow of argon (100 cm^3/min) saturated with decarbonated water through the sample at room temperature during 72 h. This sample was denoted as HT-CNFrg.

The bulk hydrotalcite was activated by either thermal decomposition or by thermal decomposition followed by rehydration in liquid phase as previously described for the supported samples. The obtained samples were denoted as HTc and HTr, respectively.

Bulk HT (Mg/Al of 2) from SASOL (PuralMg61HT) was used for the self-condensation reaction of acetone to diacetone alcohol after activation by heat treatment (HT oxide) or after heat treatment follow by gas phase rehydration (HT rehyd) performed as described above.

2.2. Characterization

Mg and Al elemental chemical analyses of the bulk samples were obtained by ICP analysis using an ICP-Spectro Arcos after the samples had been dissolved in HNO_3. Specific surface areas were determined by nitrogen adsorption at 77 K using a Quadrasorb SI equipment. Samples were previously degassed in situ at 393 K under vacuum. Surface areas were calculated using the Brunauer–Emmet–Teller (BET) methods over a p/p_0 range where a linear relationship was maintained. X-ray diffraction (XRD) powder patterns were collected on a Siemens EM-10110BU diffractometer model D5000 fitted with a Cu Kα (1.541 Å) radiation source. Data were recorded over a 2θ range of 5–70° with an angular step of 0.05° at 6 s/step which resulted in a scan rate of 0.5°/min. Patterns were identified using files from the Joint Committee on Powder Diffraction Standards (JCPDS).

The basicity measurements (volumetric CO_2 adsorption) were performed with a Micromeritics ASAP 2010 C apparatus in the range 0–100 mmHg at 300 K. Samples were previously dried at 423 K in vacuum for 24 h. After evacuation of the sample, CO_2 was dosed with small increments. The total number of accessible basic sites was determined by taking the amount of CO_2 chemisorbed at zero pressure obtained by extrapolation of the linear part of the uptake isotherm.

Thermogravimetric analysis (TGA) curves were recorded in a TGA7 thermogravimetric analyzer apparatus from room temperature to 1173 K, at a heating rate of 5 K/min.

TEM images were obtained with a JEOL 1011 TEM operating at 80 kV. Samples were dispersed in ethanol and supported on a copper grid.

2.3. Standard batch catalytic transesterification reaction

Glycerol (99%) and diethyl carbonate (DEC) (99.5%, GC grade) were purchased from Aldrich and used without any further purification. Ethanol (98%) from Aldrich was used as a solvent to characterize the products obtained. Transesterification reactions were performed in a three-neck round-bottomed flask equipped with a condenser. Typically, the flasks were charged with an excess of DEC (38.95 g) and glycerol (1.85 g) which results in a DEC:glycerol molar ratio of 17. Freshly activated catalyst (0.30 g) was added and the experiment started with mechanical stirring under argon at 403 K. Stirring was continued until the completion of the reaction. Aliquots were periodically withdrawn, filtered and quantified by GC analysis equipped with a FID detector. This was performed on a Shimadzu GC (QP 2010) with a Zebron ZW-WAX capillary column.

2.4. Recycling experiments

We investigated the reuse of the catalysts in the transesterification reaction of glycerol with DEC under the same reaction conditions that were used for the standard transesterification reaction. The reaction mixture was removed with a syringe equipped with a microfilter when the reaction had finished, leaving the catalyst in the smallest possible amount of liquid. The catalyst was then washed twice with DEC at 403 K. After that, a new charge of reactants was added to the used catalyst and the next run was performed.

2.5. Self-condensation reaction of acetone to diacetone alcohol

The self-condensation of acetone was carried out in a double-walled thermostatted batch glass reactor with a volume of 200 cm^3 at 273 K using 100 g of acetone as reactant, 6 g of iso-octane as an internal standard and 1 g of CNF supported hydrotalcite or 300 mg of bulk hydrotalcite as catalyst. The reactor was flushed with nitrogen prior to the experiment and a nitrogen atmosphere was kept over the reactor during the entire experiment to avoid exposure to air. The reactor was stirred mechanically with 1700 rpm. Aliquots of 1 cm^3 solution were taken at given times during the first 8 h of the experiments. The aliquots were filtrated through HYFLO (Sigma Aldrich) in order to remove traces of catalyst before analysis. The concentration of diacetone alcohol in the aliquots was measured using a Chrompack CP 9001 gas chromatograph equipped with an FID detector. The selectivity towards diacetone alcohol (DAA) was in all cases high and only traces of other products could be observed in the chromatograms. The activity could thus be expressed in terms of formation on DAA.

3. Results and discussion

3.1. Characterization of the catalysts

To confirm the Mg/Al molar ratio of bulk hydrotalcites, ICP analysis of samples was performed. The as-synthesized and rehydrated samples, HTas and HTr, presented Mg/Al molar ratios very close to that used in solution during the preparation with the values i.e., 2.09 and 2.05, respectively.

Fig. 1 shows the normalized XRD patterns of the supported materials at different stages of the synthesis as well as after their use in the transesterification reaction. All the samples presented diffraction lines from the presence of hydrotalcite and the CNF support. The most intense line at $2\theta \approx 27°$ corresponds to the diffraction of the CNF (graphite, JCPDS 01-075-1621). The (003) plane of hydrotalcite can be distinguished at $2\theta \approx 12°$. For the supported samples this reflection is broader compared to that for the bulk hydrotalcite [20]. This indicates that the number of HT platelets stacked on top of each other the supported hydrotalcite is lower than that of the bulk hydrotalcite. After rehydration in absence of CO_2, the original layered HT structure was recovered (due to the "memory effect") as expected [36]. However, for the rehydrated samples a slight peak broadening at $2\theta \approx 12°$ (plane (003)) was observed especially for the sample rehydrated in liquid phase (HT-CNFrl). This shows that the number of HT platelets stacked on each other is lower or that the platelets are less ordered in the rehydrated samples over the parent sample. For the spent catalysts the relative intensity of the characteristic (003) peaks of HT with respect to the most intense graphite reflection ($2\theta \approx 27°$) was decreased in the rehydrated samples. This fact could be indicative of a loss of crystallinity.

Representative TEM images of as synthesized and rehydrated samples (HT-CNFas, HT-CNFrl and HT-CNFrg, respectively) are given in Fig. 2. TEM analysis of HT-CNF revealed well-distributed

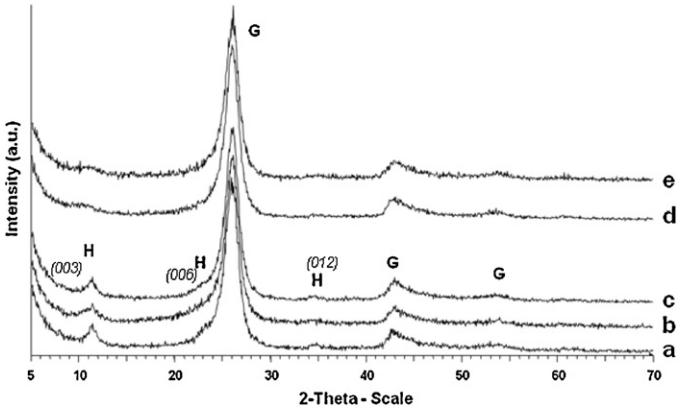

Fig. 1. X-ray diffraction patterns of (a) HT-CNFas; (b) HT-CNFrl; (c) HT-CNFrg; (d) HT-CNFrl after 1 run and (e) HT-CNFrg after 1 run. (H) represents the hydrotalcite phase and (G) represents the graphite phase.

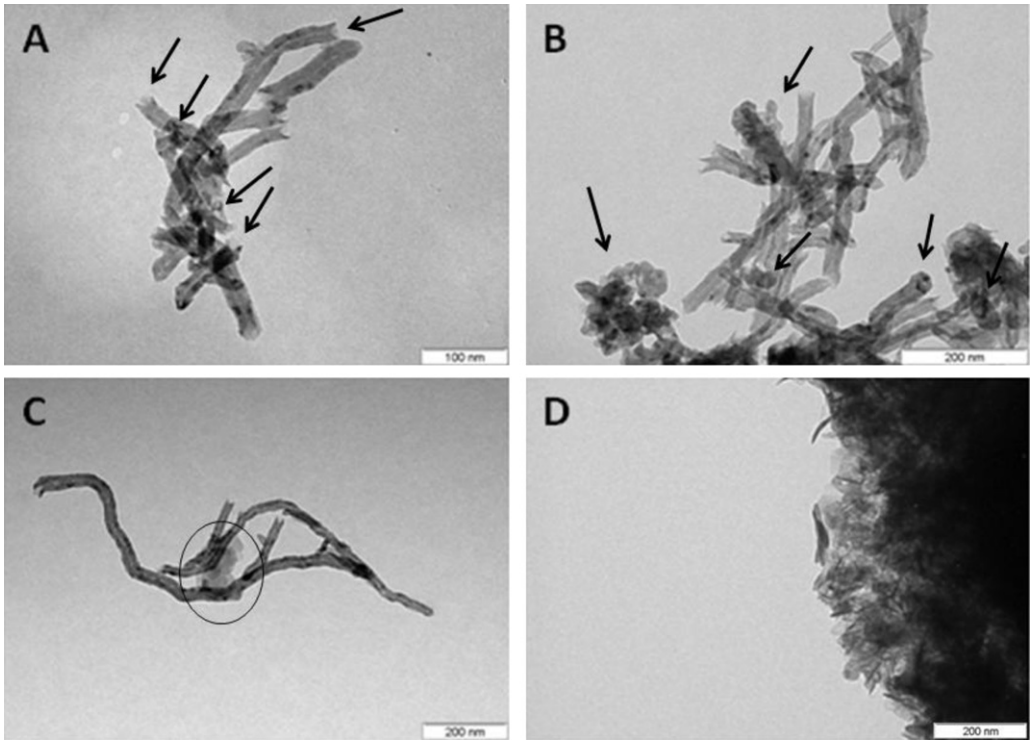

Fig. 2. TEM images of (A) HT-CNFas; (B) HT-CNFrg; (C) and (D) HT-CNFrl.

small hexagonal HT crystallites present on the carbon nanofibers and no isolated hydrotalcites separated from the fibers were observed. Some differences in morphology were observed for the sample rehydrated in liquid phase (HT-CNFrl) and larger crystallites/precipitates were found. It seems that rehydration in liquid phase results in a dissolution/recrystallization processes and apparently parts of the HT can migrate over the carbon nanofiber surface during the process. No leaching of Mg and/or Al ions was, however, observed by ICP of the water after the reconstruction in liquid phase, showing that the metal oxides remain on the support.

Specific surface area, pore volume and pore distribution of the supported hydrotalcites are summarized in Table 1. The specific surface area of the mesoporous carbon nanofiber support samples is 160–170 m^2/g. This is lower than that of the parent (190 m^2/g). This indicates that the pores might be partially filled with HT. N_2 physisorption analyses of the used samples showed that the specific surface area and the pore volume remain almost identical. The BET specific surface area for the bulk hydrotalcite (141 m^2/g and 20 m^2/g for calcined and rehydrated hydrotalcite, respectively) was in accordance with those reported in the literature [37].

To determine the amount of water present in the sample TGA was used. Fig. 3 shows the TGA results for the supported samples HT-CNF, HT-CNFrl and HT-CNFrg. The supported hydrotalcites presented two weight loss steps during the decomposition in N_2 atmosphere as expected for hydrotalcite materials. First, the removal of physisorbed and interlayer water is observed at temperatures up to 473–483 K. Then, the dehydroxylation of the layers and the decarbonation of the as-synthesized sample or dehydroxylation of the interlayer hydroxyl anions of rehydrated samples are taken place above 573 K [23,37]. The first weight loss was greater in the sample rehydrated in liquid phase than in the sample rehydrated in gas-phase (2.2% against 1.0%, respectively), which suggests that the former has more adsorbed water molecules.

TGA analyses of supported HT in O_2 were performed to calculate the loading of hydrotalcite on the CNF support (Table 1). Loading of 12% of hydrotalcite as aimed for in the synthesis was found in

Table 1
Physico-chemical properties of the different materials.

Catalyst	S_{BET} ($m^2 \cdot g^{-1}$)	Pore volume ($cm^3 \cdot g^{-1}$)	HT loading (wt%)
CNF	190	0.45	–
HT-CNFas	172	0.33	12
HT-CNFc	175	0.34	–
HT-CNFrl	173	0.35	12
HT-CNFrg	164	0.34	12
$HT\text{-}CNFc_{used}$	167	0.33	–
$HT\text{-}CNFrl_{used}$	166	0.35	–
$HT\text{-}CNFrg_{used}$	159	0.34	–

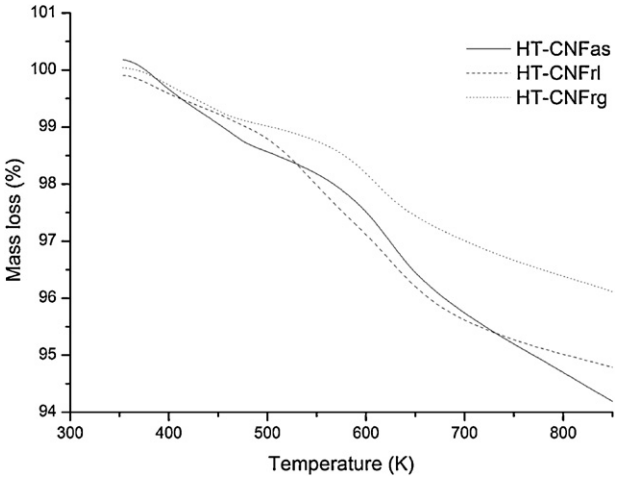

Fig. 3. Thermogravimetric analyses of supported hydrotalcites HT-CNFas, HT-CNFrl and HT-CNFrg.

Table 2
Initial reaction rates for transesterification of glycerol with DEC with the HT catalysts under the same standard conditions.

Catalyst	CO_2 adsorption (mmol $g^{-1}{}_{HT}$)	Initial rate[a] (mmol Gly $g^{-1}{}_{cat}$ h^{-1})	Initial rate (mmol Gly $g^{-1}{}_{HT}$ h^{-1})	TOF[b] (s^{-1})
HTc	0.118	18×10^{-2}	18×10^{-2}	4.2×10^{-4}
HTr	0.123	3×10^{-2}	3×10^{-2}	6.7×10^{-5}
HT-CNFc	0.445	6	53	3.3×10^{-2}
HT-CNFrl	0.358	0.4	3	2.3×10^{-3}
HT-CNFrg	0.370	0.8	7	5.3×10^{-3}

[a] Values are given over the first 60 min.
[b] Turn over frequency calculated as mol of glycerol converted per second and units of CO_2 adsorbed.

HT-CNF as well as in both rehydrated samples (HT-CNFrl and HT-CNFrg).

CO_2 was used as probe molecule to obtain information about the number of base sites in the samples (Table 2). The amount of CO_2 adsorbed on all the supported catalysts ranges from 0.370 to 0.445 $mmol_{CO_2} \cdot g^1_{HT}$, a factor 3–4 times higher than that found for bulk hydrotalcites ~0.12 $mmol_{CO_2} \cdot g^1_{HT}$. This is in accordance with earlier studies of hydrotalcites and carbon nanofiber supported hydrotalcites [31,34,35].

3.2. Catalytic results

The transesterification reaction of glycerol with diethyl carbonate over HT-CNF samples and unsupported hydrotalcites was studied. The possibility of diffusional limitations was ruled out based on the calculated Thiele modulus modified by Weisz [38].

$$\Phi = \frac{v\rho R^2}{(\mathrm{Deff} C_0)}$$

where v is the rate (mol s^{-1} g^{-1}), ρ is the catalyst density (1.5 g cm^{-3}), R the radius of the catalyst particles (here 0.075 mm), C_0 the concentration of glycerol (5×10^{-4} mol cm^{-3}), and Deff the diffusion coefficient (taken as 10^{-5} cm^2 s^{-1}). The low values of Weisz modulus calculated for supported hydrotalcites (about 0.03) indicated the absence of diffusion limitations. Therefore, the effect of mass transfer did not limit the reaction.

Fig. 4 and Table 3 show the results of the catalytic performance using activated supported and bulk hydrotalcites. Carbon nanofibers themselves did not show any catalytic activity. A high activity for glycerol transesterification was found for the supported catalysts, especially the calcined sample (HT-CNFc) showed superior activities. If comparing the initial rate expressed per mol hydrotalcite of heat treated supported HT sample, HT-CNFc (53 mmol Gly·$g^{-1}{}_{HT}$·h^{-1}), with the bulk, HTc (0.18 mmol Gly·$g^{-1}{}_{HT}$·$h^{-1)}$ the supported material is almost a factor 300 better than the bulk. Furthermore, this sample showed significant higher catalytic activity than traditional transesterification catalysts such as K_2CO_3 which first achieves full conversion (97%) of glycerol conversion after 6 h under the same reaction conditions [20,39], while the HT-CNFc reached this level within 90 min.

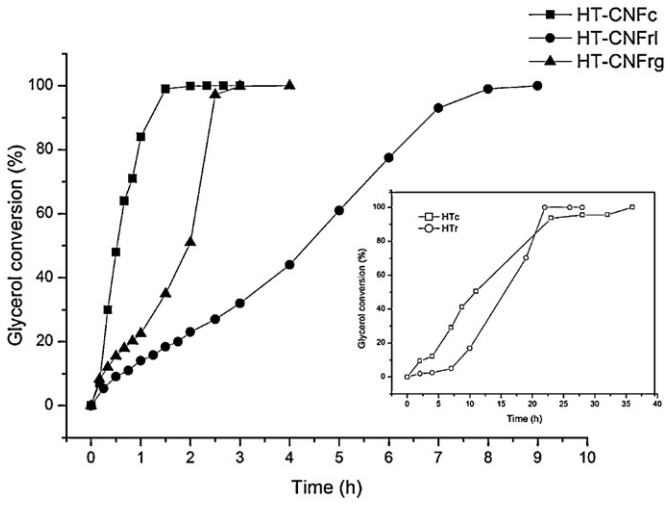

Fig. 4. Catalytic behaviour of the different catalysts at 403 K and a glycerol: DEC molar ratio 1:17. Insert: Catalytic behaviour of bulk hydrotalcites under the same standard conditions.

The bulk calcined HT showed higher initial rate than that of the rehydrated bulk catalyst, respectively $15 \cdot 10^{-2}$ and $3 \cdot 10^{-2}$ mmol Gly·$g^{-1}{}_{cat}$·h^{-1} (Table 2). The glycerol conversion seems to occur with an induction period for the bulk materials (Fig. 4) where the 'delay' for the rehydrated sample is more pronounced than for the heat treated. This behaviour may be due to the great hydrophilic character of the hydrotalcite surface in the rehydrated form, since more water is present in this catalyst. After this initial period, the glycerol conversion increased greatly to form a plateau at almost full glycerol conversion reach by~ 22 h of reaction.

When looking closer into the behaviour of the supported catalysts the rehydrated catalyst, HT-CNFrl, showed a noteworthy lower activity with an initial rate of 4 $mmol_{gly}$ $g^{-1}{}_{HT}$ h^{-1} and needed 8 h to achieve full glycerol conversion compared to 1.5 h reaction time necessary to reach full conversion in the case of the calcined HT-CNFc catalyst. Moreover, the consecutive transesterification of glycerol carbonate to yield glycerol dicarbonate occurred in a very low percentage (3% of glycerol dicarbonate after 8 h of reaction) for the liquid phase rehydrated sample. The catalyst having the lowest activity was thus the most selective to the first product of the transesterification reaction, i.e., glycerol carbonate. The gas-phase rehydrated sample HT-CNFrg also exhibited lower initial activity in the transesterification of glycerol than the HT-CNFc catalyst. However, the initial rate is twice as high as for the liquid phase rehydrated catalyst (HT-CNFrl) and a total glycerol conversion was observed after 3 h of reaction. The greater activity of HT-CNFrg with respect to HT-CNFrl is also reflected in the increased selectivity to the second product of condensation (≈ 21% after 3 h of reaction). The poor activity of HT-CNFrl is tentatively attributed to the higher amount of water contained in that sample, as indicated by TGA analysis. This is in accordance with a previous study performed in our group [20] showing that though Brønsted basicity presented by rehydrated hydrotalcites is more favourable for transesterification reactions than Lewis basicity (presented in the parent mixed oxides) a very low activity for samples containing high amounts of water (HTr2) is observed also resulting in an induction period in the beginning of the reaction (as observed in Fig. 4). This can be explained by the high solubility in water of glycerol while DEC is not soluble in water. As a result cannot easily reach the active sites. Moreover, free water might even result in the hydrolysis of glycerol carbonate driving the equilibrium of the reaction again towards the formation of glycerol.

The adsorption of reactants, influenced by the polarity of the catalyst, is therefore determining the catalytic activity. For the

Table 3
Catalytic behaviour of the different materials tested in the transesterification of glycerol under standard conditions.

Entry	Catalyst[a]	Reaction time (h)	Glycerol converted (%)[b]	Yield GC (%)[b]	Yield GDC (%)[b]
1	HTc	32	96	65	31
2	HTr	22	100	75	25
3	CNF	8	–	–	–
4	HT-CNFc	2	100	58	42
5	HT-CNFrl	8	99	96	3
6	HT-CNFrg	3	100	79	21
7	HT-CNFc[c,d]	5[c]	99[c]	47[c]	52[c]
		7[d]	99[d]	87[d]	12[d]

[a] All the catalysts were tested under the same reaction conditions (0.3 g of catalyst, Gly:DEC 1:17, 403 K and 1 atm).
[b] Conversion and yields were determined by GC-FID.
[c] Conversion and yields found after a second run.
[d] Conversion and yields found after a third run.

supported samples we speculate that the heat treatment removed a significant amount of oxygen groups from the CNF support [40] thus making the support less polar. This in turn might favour the adsorption of the DEC on a HT-CNF catalyst compared to a bulk HT material resulting in an increase of the reaction rate. The polarity difference between bulk and supported samples is assumed to play a major role for the catalyst performance since it is obvious from Table 2 that the number of base sites (though a factor 3 higher for supported samples than for bulk) cannot explain the difference in activity between bulk and supported samples of a factor 300. When considering the impact of polarity on the catalytic performance it is interesting to notice that Tichit et al. [24] previously reported that rehydrated MgAl hydrotalcites were more active in the catalytic acetone self-condensation than the mixed oxide. For a different reaction the opposite performance pattern was thus observed compared to the results reported for the transesterification reaction here. In view of Tichits results a series of experiments were performed using the supported catalysts in the acetone self-condensation to clarify if a similar behaviour was found as for the reported bulk materials. In Fig. 5 the formation of diacetone alcohol versus time is plotted for HT-CNFc, HTCNFrg, HT oxide, HT rehyd.

For both supported and unsupported HT catalyst we find (Fig. 5) that the rehydrated catalyst is more active than the mixed oxide in the self-condensation reaction, which is in accordance with Tichits findings for the bulk system.

This shows very clear that the performance of the mixed oxide and the HT catalysts in these two base-catalyzed reactions is very different. In the case of transesterification of glycerol, the higher amounts of water in the supported catalysts have shown to produce a negative effect on the catalytic activity due to the lack of solubility of one of the reactant, DEC, as discussed above. Such an effect is not expected in the self-condensation of acetone, since acetone is soluble in water.

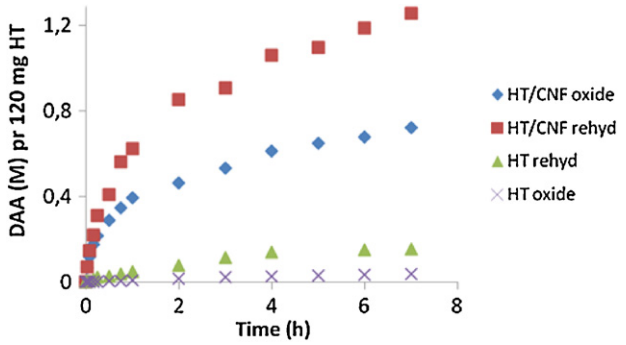

Fig. 5. Self-condensation of acetone with diacetone alcohol at 0 °C using 1 g of supported catalyst/300 mg bulk catalyst and 100 g of acetone.

3.3. Stability of the catalysts

An important aspect of heterogeneous catalysts is their stability or reusability in batch reactors. In the transesterification reaction the highest stability was observed for the HT-CNFc sample. A slight loss of activity was, however, observed in every consecutive run (see Fig. 6). Total glycerol conversion was reached in the first run in 90 min, dropping to 85% and 80% for the second and the third run. However, remarkable changes were observed in the selectivity. The selectivity to the undesired second product of transesterification (glycerol dicarbonate, GDC) was higher in the first run and diminished abruptly with every run until no glycerol dicarbonate is obtained in the third run. This change in selectivity is indicative of some deactivation of the catalyst and could be attributed to a strong adsorption of side products or a loss of HT phase from the HT-CNF samples during the reaction. However, the consequent of this is that the yield of the desired product, GC, remains very high during the consecutive runs (57, 82 and 81% of yield after 90 min of reaction for first, second and third run, respectively), which is a greater advantage than the smaller loose of overall conversion.

One experiment was performed in order to see if some HT phase was dissolved/leached during the reaction and to investigate if there was any activity of the potentially dissolved HT phase. For this purpose the HT-CNFc catalyst was removed from the reactor after 60 min of reaction time. As illustrated by the reaction profile in Fig. 7, the conversion of glycerol stopped after the removal of the catalyst. Moreover, the composition of the products did not change. These results confirm that there was no homogeneous catalytic contribution to the catalytic activity observed. Moreover, no

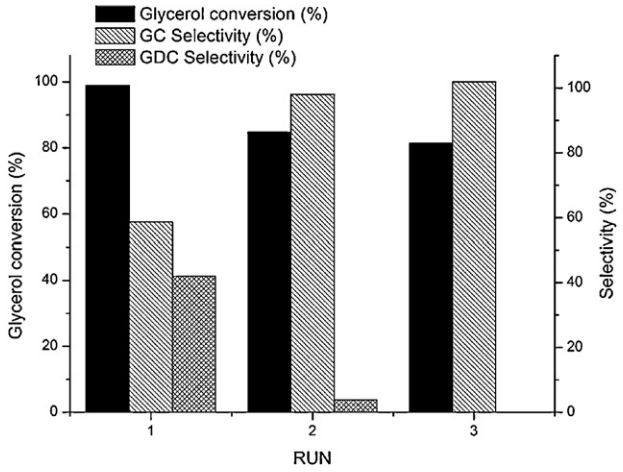

Fig. 6. Catalytic performance of HT-CNFc catalyst in three consecutive runs under standard reaction conditions.

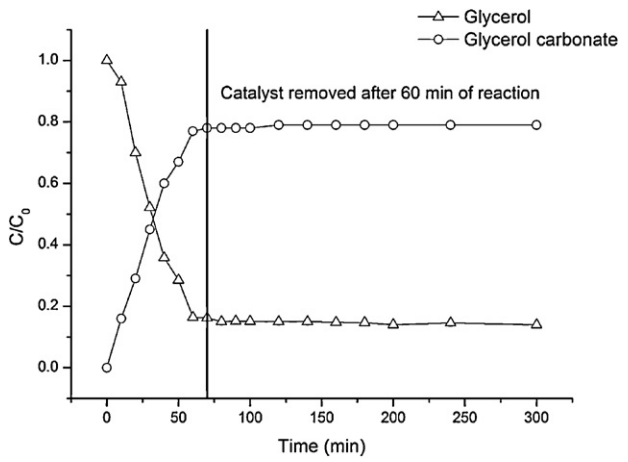

Fig. 7. Transesterification profiles for HT-CNFc and removing of catalyst. Reaction was performed at 403 K and with a glycerol: DEC molar ratio 1:17.

traces of Mg or Al were detected in the liquid phase at the end of this experiment, showing that no leaching takes place. Furthermore, BET surface areas, as well as pore distribution of the catalyst remained practically identical after the transesterification reaction indicating the absence of pore blockage by fouling. These results indicate that the main cause of deactivation is due to a strong adsorption of some products on the surface poisoning the catalyst and might be solved by a re-activation procedure after a certain number of catalytic runs if desired.

4. Conclusions

Activated hydrotalcites supported on carbon nanofibers have been tested as solid base catalysts in the transesterification of glycerol with diethyl carbonate to obtain glycerol carbonate under mild conditions. These materials exhibited much greater catalytic activity in the transesterification of glycerol with DEC than bulk activated hydrotalcites. In particular, HT-CNFc showed a catalytic activity almost 300 times higher than that showed by bulk catalyst (HTc). The high activity in combination with the fact that HT-CNFc) could be reused in three consecutive runs without significant loss of activity make it a promising candidate as a solid catalyst for the transesterification reaction and would be able to replace other catalysts working in homogeneous phase such as potassium carbonate which present similar or lower performance under the same catalytic conditions.

Large amounts of water in rehydrated HT samples resulted in less activity and a long induction period in the transesterification reaction. The catalyst rehydrated in gas phase revealed a catalytic activity higher than the catalyst rehydrated in liquid phase, probably due to relocation/migration of the active phase in the latter. Thus, the reconstruction method of the hydrotalcite has a great influence on the catalytic behaviour of the final catalyst. The low-hydration degree of the mixed oxide together with the hydrophobicity of the CNF support led to the enhancement activity of the transesterification reaction for the HT-CNFc compared to the rehydrated samples. The opposite trend was observed in the acetone self-condensation reaction where the rehydrated sample was considerably better than the oxide. This indicates that polarity of the catalyst and polarity of different reactants is very important to consider in the optimization of solid base catalysts for a given reaction. Insight in these matters might make it possible to design more efficient catalysts in the future.

Acknowledgements

Authors acknowledge the financial support from the Spanish Government's Ministry of Science and Technology (project CTQ2006-08196 and CTQ2008-03043-E, ACENET).

References

[1] M. Pagliaro, R. Ciriminna, H. Kimura, M. Rossi, C. Della Pina, Angewandte Chemie International Edition 46 (2007) 4434.
[2] K. Klepácová, D. Mravec, M. Bajus, Applied Catalysis A-General 294 (2005) 141.
[3] J. Barrault, J.M. Clacens, Y. Pouilloux, Topics in Catalysis 27 (2004) 137.
[4] J.A. Melero, R. Van Grieken, G. Morales, M. Paniagua, Energy and Fuels 21 (2007) 1782.
[5] S.H. Chai, H.P. Wang, Y. Liang, B.Q. Xu, Journal of Catalysis 250 (2007) 342.
[6] A. Corma, G.W. Huber, L. Sauvanaud, P. O'Connor, Journal of Catalysis 250 (2007) 307.
[7] R.R. Soares, D.A. Simonetti, J.A. Dumesic, Angewandte Chemie International Edition 45 (2006) 3982.
[8] M. Bandres, A., Deswartvaegher, C.P. De, Patent WO2007/080172.
[9] M. Notari, F. Rivetty, Patent WO2004/052874.
[10] D. Herault, A., Eggers, A., Strube, J. Reinhardt, Patent DE 10110855.
[11] P. Traupe, M. Maurer, S. Moeller, M. Yung, A. Hallmann, Natsch, Patent DE 10323703.
[12] A. Bher, J. Eilting, K. Irawadi, J. Leschinski, F. Lindner, Green Chemistry 10 (2008) 13.
[13] A.S. Kovvali, K.K. Sikar, Industrial & Engineering Chemistry Research 41 (2002) 2287.
[14] H.S. Bevinakatti, A.G. Waite Frank, J. WO 2008/142374 A1 (2008).
[15] G. Rokicki, P. Rakoczy, P. Parzuchowski, M. Sobiecki, Green Chemistry 7 (2005) 529.
[16] J. Guan, Y. Song, Y. Lin, X. Yin, M. Zuo, Y. Zhao, X. Tao, Q. Zheng, Industrial & Engineering Chemistry Research 50 (2011) 6517.
[17] Z. Mouloungui, J.W. Yoo, C.A. Gachen, A. Gaset and G. Vermeersch, EP0739888.
[18] J.R. Ochoa-Gómez, O. Gómez-Jiménez-Abesraturi, B. Maestro-Madurga, A. Pesquera-Rodríguez, C. Ramírez-López, L. Lorenzo-Ibarreta, J. Torrecilla-Soria, M.C. Villarán-Velasco, Applied Catalysis A-General 366 (2009) 315.
[19] W.T. Reichle, Solid State Ionics 22 (1986) 135.
[20] M.G. Álvarez, R.J. Chimentão, F. Figueras, F. Medina, Applied Clay Science 5 (2012) 16.
[21] A. Takagaki, K. Iwatani, S. Nishimura, K. Ebitani, Green Chemistry 12 (2010) 578.
[22] Layered Double Hydroxides, Eds. X. Duan, D.G., Evans, Springer, Germany (2006).
[23] V. Rives, Ed., Layered Double Hydroxides: Present and Future, Nova Sci. Pub., Inc., New York (2001), and references therein.
[24] D. Tichit, M. Naciri Bennani, F. Figueras, R. Tessier, J. Kervennal, Applied Clay Science 13 (1998) 401.
[25] A. Guida, L.M. Hassane, D. Tichit, F. Figueras, P. Geneste, Applied Catalysis A-General 164 (1997) 251.
[26] M.L. Kantam, B.M. Choudary, C.V. Reddy, K.K. Rao, F. Figueras, Chemical Communications 9 (1998) 1033.
[27] M.J. Climent, A. Corma, S. Iborra, J. Primo, Journal of Catalysis 151 (1995) 60.
[28] B.M. Choudary, M.L. Kantam, C.R. Reddy, K.K. Rao, F. Figueras, Journal of Molecular Catalysis A 146 (1996) 279.
[29] G.S. Macala, A.W. Robertson, C.L. Johnson, Z.B. Day, R.S. Lewis, M.G. White, A.V. Iretskii, P.C. Ford, Catalysis Letters 122 (2008) 205.
[30] B. Veldurthy, J.M. Clacens, F. Figueras, Journal of Catalysis 229 (2005) 237.
[31] J.C.A.A. Roelofs, D.J. Lensveld, A.J. van Dillen, K.P. de Jong, Journal of Catalysis 203 (2001) 184.
[32] S. Abelló, F. Medina, D. Tichit, J. Pérez-Ramírez, Y. Cesteros, P. Salagre, J.E. Sueiras, Chemical Communications (2005) 1453.
[33] R.J. Chimentão, S. Abelló, F. Medina, J. Llorca, J.E. Sueiras, Y. Cesteros, P. Salagre, Journal of Catalysis 252 (2007) 249.
[34] F. Winter, A. Jos van Dillen, K.P. de Jong, Chemical Communications (2005) 3977.
[35] F. Winter, V. Koot, A.J. van Dillen, J.W. Geus, K.P. de Jong, Journal of Catalysis 236 (2005) 91.
[36] S. Miyata, Clays and Clay Minerals 28 (1980) 50–56.
[37] F. Cavani, F. Trifiro, A. Vaccari, Catalysis Today 11 (1991) 173.
[38] P.B. Weisz, Science 179 (1973) 433.
[39] M.G. Álvarez, A.M. Segarra, S. Contreras, J.E. Sueiras, F. Medina, F. Figueras, Chemical Engineering Journal 161 (2010) 340.
[40] M.L. Toebes, J.M.P. van Hees Wijk, J.H. Bitter, A.J. van Dillen, K.P. de Jong, Carbon 42 (2004) 307.